Journal of Membrane Science & Research

journal homepage: www.msrjournal.com

Research Paper

Spiral Hollow Fiber Membrane Contactor for Chromium (VI) Removal from Aqueous Sluotion

Narimene Zeghouati [1], Said Bey [1,*], Abdelatif Belamri [2], Alberto Figoli [3], Alessandra Criscuoli [3], Mohamed Benamor [1], Enrico Drioli [3]

[1] *Laboratory of Membrane Processes and Separation and Recovery Techniques, Faculty of Technology, University of Bejaia, Algeria*
[2] *Laboratory of Mechanics, Materials and Energetics, Faculty of Technology, University of Bejaia, Algeria*
[3] *Institute on Membrane Technology (ITM-CNR),Via P.Bucci 17/C,87030 Rende (CS)- Italy*

Article info

Received 2024-01-25
Revised 2024-07-21
Accepted 2024-10-21
Available online 2024-10-21

Keywords

Cr(VI)
Aliquat-336
Membrane contactors
Spiral hollow fiber module

Highlights

- Synthesis and characterization of PSF-based hollow fibers by dry/wet phase inversion
- A spiral hollow fiber membrane module was developed for efficient removal of Cr (VI)
- The spiral hollow fiber membrane contactor achieved 95% efficiency in Cr (VI) removal

Graphical abstract

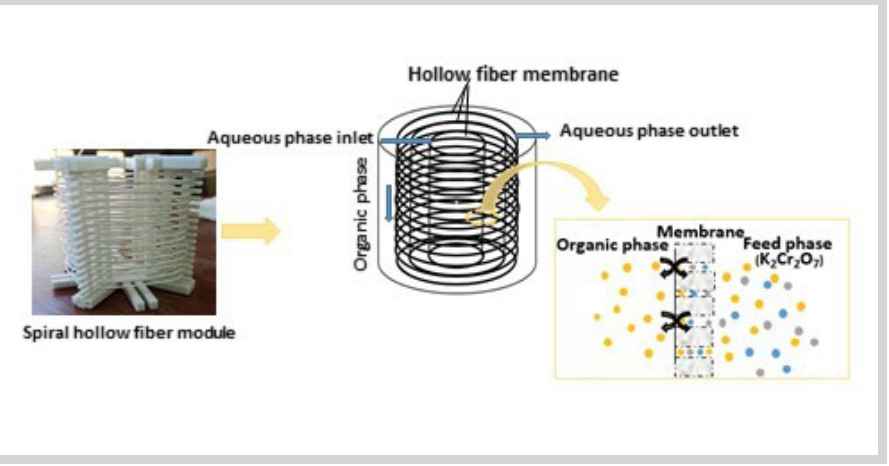

Abstract

Chromium (VI) was successfully removed, from aqueous solution, using a new spiral hollow fiber module. It consists of three stages supporting a single hollow fiber based on polysulfone (PSF). Fibers were prepared using a dry/wet phase inversion technique, and several factors, including the type of coaxial coagulant, its injection rate, and the concentration of polymer, were examined. A number of techniques were used to characterize the hollow fibers regarding porosity, morphology, wettability, and mechanical strength. Asymmetric structure was obtained with a finger-like structure. This latter disappears slightly using additives in the coaxial coagulant. However, no significant effect of the increase in polymer concentration on the morphology of membranes. The prepared hollow fibers were tested for Cr(VI) recovery using Aliquat-336 as extractant in the designed spiral hollow fiber contactor. The results indicated that the new system could be a promising technique in the field of membrane contactors for metal ion separation with a separation efficiency of 95% and a flux of 3.8 µmol/m^2.s.

1. Introduction

For more than a decade, chromium contamination has garnered global attention because of its bioaccumulation, high toxicity, and carcinogenic properties. It comes primarily from industrial processes. Chromium (III) Trivalent and Chromium (VI) Hexavalent are two of the most stable oxidation forms of chromium. Chromium (III) is a necessary trace element for the organism, whereas chromium (VI) is highly poisonous and readily absorbed and accumulates in the human body [1]. Excessive exposure to this metal can lead to irreversible effects in humans and other living organisms. Chromium (VI) significantly contributes to the development of cancerous and non-cancerous tumors [2] and can cause various health issues, including liver damage, skin rashes, kidney disorders, respiratory problems, and lung cancer [3]. Due to health and environmental concerns, the World Health Organization

* Corresponding author: Said.bey@univ-bejaia.dz (S. Bey)
DOI: 10.22079/jmsr.2024.2021108.1649

has established a maximum allowable limit of 0,5 ppm for Chromium (VI) in wastewater [4].

Therefore, removing Cr(VI) presents a worldwide challenge. A range of methods has been proposed. Jia et al. [5] reported that 95% of Cr(VI) was successfully removed in 3 min, using polyamine modified carbon nanotubes (PA-CNTs) as adsorbents. Ying et al [6] also studied chromium extraction from wastewater using an amide as extractant and achieved a total chromium recovery of 95.40%. Dermentzis et al. [7] showed that 99.9% of Chromium (VI) was removed from real electroplating effluents, using chemical coagulation and an electrocoagulation process.

Most of these techniques have drawbacks, namely the high cost of equipment and the formation of secondary pollutants. Consequently, there is a need to develop an economical and efficient treatment process for chromium removal. Membrane processes are of particular interest because of their many advantages, they offer high selectivity, improved efficiency and low energy consumption **[8]**, and can replace several conventional separation methods [9]. Various types of membranes are employed for removing of Cr(VI), such as polymer inclusion membranes [10] and liquid membranes [11].

Membrane contactors have attracted significant attention in the treatment of gases and liquids. They are devices that allow mass transfer by providing non-dispersive contact between phases. In particular, hollow fiber membrane technology is often adopted, which is the most widely used configuration due to its large contact area per unit volume, high efficiency, and flexibility [12]. Hollow fiber contactors can be used in different applications and industries, such as chemical, pharmaceutical, and petrochemical industries; wastewater treatment; pollutant removal [13]; acid gas absorption [14]; gas humidification [15]; space missions to recycle wastewater [16]; and fatty acids removal [17]. They are also utilized as artificial lungs for patients with various lung diseases [18].

However, shorter membrane lifetime and lower productivity are the main drawbacks of membrane separation processes [19]. Several researches have been done for the design of efficient membrane modules with optimized geometries to enhance permeation and reduce concentration polarization. The efficiency of a module depends on the intrinsic membrane separation properties, and also on the hydrodynamics of the fluids inside the module [12]. For instance, changing the membrane's arrangement results in flow instability and secondary streams (Dean vortices), which are generated by centrifugal force [20]. This reduces the concentration gradient and enhances mass transfer. The transfer of gases in the blood was the first application of these secondary fluxes [21].

Several investigations have been conducted about the design of hollow fiber module geometries. Coiled hollow fiber module was developed by Liu et al. [22]. At a specific wind angle, hollow fiber membranes were wound around a stainless steel tube. When compared to the traditional straight module, they discovered that the mass transfer on the tube and shell sides was better. Schlosser and Sabolova [23] used U-shaped hollow fiber bundles in a three-liquid-phase contactor for the pertraction of dimethyl cyclopropane carboxylic acid (DMCCA) and phenol. Chen et al. [20] evaluated the performance of four membrane contactors with different geometries: curved to 90 degrees, meandering, knotted, and helical. The membrane contactor used consisted of an inner tube, a concentric outer tube, and a PTFE-based membrane. Kong et al. [24] studied helical and straight hollow fiber modules for water deoxygenation. To create the helical hollow fiber membrane bundle, three straight fibers were twisted together, resulting in a uniform step and curvature diameter. The deoxygenation rate of the helical hollow fibers was twice as high as that of the straight hollow fibers. Ghogomu et al. [25] used linear, helical, twisted, and sinusoidal modules with hollow fiber ultrafiltration (UF) membranes and tested them on bentonite suspensions. Sofiya et al. [26] investigated the separation of propionic, formic and acetic acids from an aqueous solution using three membrane modules made of PVDF, PES, and PSF. These modules were arranged vertically with a co-current operation.

In the first part of this study, the PSf/PVP/DMAc system was investigated. Several parameters and their effects on the morphology and properties of hollow fibers were examined, namely the type of coaxial coagulant and its injection rate. In the second part, the prepared hollow fibers were applied in a liquid-liquid extraction system using a new spiral hollow fiber membrane contactor for the removal of chromium (VI) from the aqueous solution.

2. Experimental

2.1. Materials

Polysulfone P-3500 (PSF) was used as base polymer, Dimethylacetamide (DMAc) was provided by Carlo ERBA Reagents, and used as solvent to prepare the polymer solution, Polyvinylpyrolidone Luviskol® K17 (PVP- K17) was purchased from BASF, and Ethanol (EtOH) was obtained from Sigma Aldrich. Potassium dichromate ($K_2Cr_2O_7$) was purchased by PROLAB to prepare the aqueous solution, Aliquat 336 ($[CH_3(CH_2)_7]_3$ NCH_3Cl), Kerosene, and 1-Octanol were used to prepare the organic phase, all supplied by Sigma-Aldrich. Sodium hydroxide (NaOH), Hydrochloric acid (HCl), and Sodium chloride (NaCl) were also purchased from Sigma-Aldrich.

2.2. Preparation of hollow fibers based on polysulfone

The polymeric solution was prepared by dissolving 20 wt.%, 25 wt.%, and 30 wt.% of polysulfone and polyvinylpyrrolidone in dimethyl acetamide. PVP was used as an additive with distilled water for pore formation. The doped polymeric solution was mixed using a mechanical blender and heated to 85°C to obtain a homogeneous solution and left to stand overnight for degassing. After degassing, the solution was transferred to a conical tank pressurized with nitrogen gas, connected to the spinneret with internal (di) and external (de) diameters of 600 µm and 1600 µm, respectively. Different liquids were prepared and introduced into the central axis of the spinneret using a peristaltic pump. The preparation conditions for hollow fibers are summarized in Table 1. Several parameters were studied, namely the injection rate and the composition of the coagulants inside the fibers (central axis of the spinneret). The fibers were obtained in a rotary bath containing distilled water at 25°C. The recovered fibers were washed in distilled water at 50°C, and stored in a 40% glycerol solution to preserve their properties. Washing the fibers with hot water removed the PVP remaining in the polymer matrix, thereby obtaining a porous structure. After drying, the fibers were characterized using different techniques. A schematic representation of the hollow fiber membrane preparation process is described in our previous study [27]. At 30 % wt. of polysulfone, the viscosity of the polymeric solution is high and requires heating above 80 °C for complete dissolution. Hence, membranes were not prepared at this concentration.

2.3. Viscosity measurement of polymeric solutions

Before preparing the fibers, a study of polymeric solutions' viscosity is necessary. A Brookfield DVIII ultra viscometer was used for this purpose. These viscosity measurements were used to identify the optimum concentration of the polymer solutions studied, in order to achieve an appropriate composition for optimal fiber preparation. For the PSF/ PVP / DMAc system, polymeric solutions were prepared at different concentrations of the polymer (20 wt.%, 25 wt.%, 30 wt.%) and PVP (0 wt.%, 5 wt.%, 10 wt.%, 15 wt.%). The viscosity measurement was conducted at different concentrations of polymer and PVP, and at three temperatures: 50 °C, 60 °C, and 70 °C.

Table 1
Conditions for preparing hollow fiber membranes based on PSF.

Fiber n.	Polymer PSF	Additive	Temperature (°C)	Coaxial coagulant Composition /Rate
1-A	20wt.%	PVP K-17 15%	50	H_2O 100%, 30 rpm
1-B				DMAc 30%, 30 rpm
1-C				EtOH 30%, 30 rpm
1-D				DMAc 30%, 50 rpm
2-A	25wt.%	PVP K-17 10%	70	H_2O 100%, 50 rpm
2-B				DMAc 30%, 50 rpm
2-C				EtOH 30%, 50 rpm
2-D				DMAc 30%, 70 rpm
2-E				DMAc 30%, 30 rpm
2-F				EtOH 30%, 30 rpm

2.4. Characterization of hollow fibers

2.4.1. Determination of the porosity

Porosity is defined as the ratio of the pore volume to the membrane's total volume. It can be computed using the gravimetric approach as explained in [28], The formula is as follows:

$$\varepsilon\ (\%) = (1 - \rho_{fiber}/\rho_{PSF}) \times 100$$

Where ρ_{fiber} and ρ_{PSF} represent the densities of the fiber and the PSF powder, respectively.

2.4.2. Determination of contact angle and pore size

The wettability of hollow fiber membranes was studied by determining the contact angle (θ) between the membrane surface and distilled water, using the Krüss drop shape analyzer. A droplet containing 0.2 µL of distilled water was applied to the membrane surface, at a temperature of 20°C. The relationship between contact angle and hydrophilicity is inversely proportional.

The fibers' average pore size was measured using a PMI capillary flow porometer (Porous Materials Inc., USA).

2.4.3. Measurement of mechanical properties

The strength of the hollow fibers was evaluated using a Zwick/Roell Z2.5 test unit. Elongation at break, tensile strength, and Young's modulus were determined. For every sample, five specimens were analyzed.

2.4.4. Morphology

Membrane morphologies were examined by scanning electron microscopy (SEM) (Quanta FENG 200, FEI Company). Membrane cross-sections were delicately fractured in liquid nitrogen, to obtain a smooth, brittle fracture. The internal surfaces and cross sections were then observed.

2.5. Description of the spiral hollow fiber contactor

Fig. 1 shows image of a new module, called a spiral hollow fiber membrane contactor designed at the laboratory scale, consisting of three stages, with a height and diameter of 9.5 cm. The module has a volume of 673 cm^3. Each stage is composed of four rectangular tubes divided into small openings of 0.3 cm, allowing the hollow fiber to pass through in a spiral geometric configuration. The hollow fiber membrane, measuring 9 meters in length, is wound around these four tubes with a pitch of 0.5 cm in each of the three stages. The ends of the membrane are sealed with epoxy resin glue to permit the aqueous feed phase to enter and exit. This membrane module is submerged in an organic phase-filled glass box.

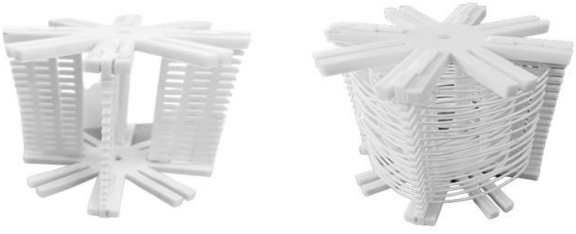

Fig. 1. Spiral hollow fiber membrane contactor.

2.6. Experimental procedure

The prepared hollow fibers were used for non-dispersive solvent extraction of chromium using the spiral hollow fiber contactor.

A diagram of the experimental setup, including the spiral hollow fiber contactor and the flow system, is shown in Fig. 2. A solution of potassium dichromate ($K_2Cr_2O_7$) with a concentration of 100 mg/l was prepared and adjusted to a pH of 4.5 using Hydrochloric acid (0.1 M). The aqueous feed phase and the organic phase, containing 20% (v/v) of Aliquat 336 (0.437 mol/l) modified with 4% (v/v) of 1-Octanol (0.253 mol/l) diluted in kerosene, with a volume of 500 cm^3, were brought into contact by passing the aqueous phase through the lumen side of the contactor using a peristaltic pump set to a flow rate of 10.8 ml/min. All experiments were run for 7 hours at a temperature of 20°C. Phase dispersion was avoided by maintaining low pressure (0.1–0.3 bar) on the aqueous phase side.

Before starting the experiment, distilled water was introduced into the hollow fiber until all system parameters stabilized. Then, the distilled water was replaced with the metal solution.

Following extraction, the chromium re-extraction process was carried out using different stripping solutions: NaOH at concentrations of 0.05 M and 0.1 M, and NaCl at 2 M. Each stripping solution was introduced into the hollow fiber membrane contactor under the same operational conditions.

Samples from the aqueous phase were analyzed using a UV-Vis spectrophotometer (Thermo Scientific Evolution 220) at a wavelength of 542 nm with diphenylcarbazide (0.02 mol/L) to determine the concentration of the samples.

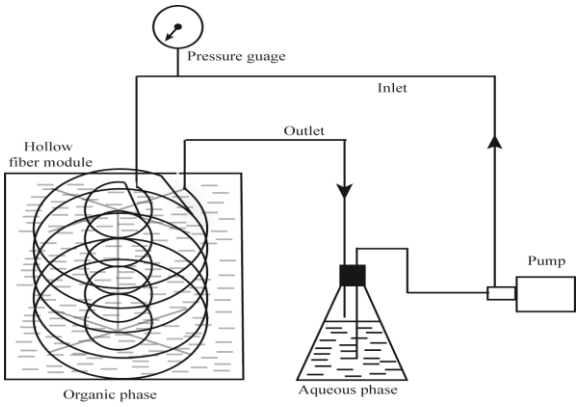

Fig. 2. Experimental setup.

3. Results and discussions

3.1. Analysis of Viscosity Results

According to the viscosity measurements of the various polymer solutions (Table 2), it emerges the following:

- The viscosity of polymeric solutions increases with the addition of PVP.
- Increasing the concentration of PSF leads to a rise in viscosity.
- Increasing the temperature decreases the viscosity of the dope solutions.

These viscosity measurements enabled us to determine the appropriate polymeric solution for spinning and to obtain high-quality hollow fibers. As a result, polymeric solutions containing 20 wt.% PSF / 15 wt.% PVP and 25 wt.% PSF / 10 wt.% PVP were found to be the most suitable for spinning. It should be noted that polymeric solutions composed of 30 wt.% PSF with 10 wt.% and 15 wt.% PVP are difficult to prepare; they require heating up to 80°C and a longer time (24 hours) to achieve clear solutions.

Mansur et al. [29] studied the PSF/PVP/NMP system for the formation of hollow fibers at different concentrations of PVP. They observed that higher concentrations of PVP raise the viscosity of the polymeric solution and delay the phase inversion process.

Furthermore, Han and Nam. [30] showed that adding PVP increases the viscosity of the polymeric solution and prevents the system's constituent parts from diffusing together. Phase separation is thus delayed as a result of the exchange between the solvent and the non-solvent being impacted during the process. In fact, at low concentrations of PVP, its addition promotes phase separation. However, at high concentrations, the viscosity increases and the delayed separation of the phases is favored.

Table 2
Viscosity measurement of PSF/PVP/DMAc solutions.

Polymer wt.%	PVP wt.%	Viscosity (cP)		
		50 °C	60 °C	70 °C
20	0 %	525.7	457.7	381.7
	5 %	1008	800	620
	10 %	1428	1058	950
	15 %	2775	457,7	1521
25	0 %	1867	1474	1364
	5 %	3389	2759	2092
	10 %	5915	4092	3553
	15 %	/	7888	5940
30	0 %	6707	5483	4259
	5 %	10838	8488	6944
	10 %	17537	16696	14032
	15 %	/	26744	22915

3.2. Morphology analysis

Figs. 3 and 4 represent the SEM images of the PSF hollow fibers prepared under different conditions. The morphologies of the membranes were examined through SEM analysis of the inner surface and the cross-section. It appears that the hollow fibers obtained are asymmetric, characterized by a microporous inner layer and a spongy outer layer. It should be noted that increasing the PSF concentration (from 20 wt.% to 25 wt.%) has no effect on the hollow fiber structure. Microvoids in the shape of channels were observed, and they did not disappear regardless of the polymer concentrations, coagulant type, or injection rate. Conversely, the use of pure water as a coagulant reveals the presence of microvoids throughout the section because of the water's penetration into the polymeric film, attributed to PSF's hydrophilic nature. As a result, a thin, more or less dense layer formed (with pores on the order of nanometer) on the inside and outside surfaces (hollow fiber 1A). The thickness of the latter increases for DMA and ethanol used at 30% (hollow fibers 1B, 1C, 1D). This can be explained by the low penetration of these two coagulants for the formation of channels until reaching the external surface. It should be noted that increasing the injection rate of the coaxial coagulant results in better coagulant penetration and the formation of channels running along the entire cross-section of the fibers (fibers 2A to 2D). However, an unexpected result was observed when the PVP concentration was reduced to 10% wt, and the PSF concentration was increased to 25 wt.%, the outer layer of the fibers remained spongy. Indeed, for the suppression of microvoids, it is judicious to increase the concentration of PVP for reducing the demixing rate, particularly in the case of hydrophilic polymers.

For Machado et al. [31] the uniformity of the microvoids particularly depends on the composition of the bath of coagulation. It was observed that with the addition of DMAc to the coagulation bath at 50%, the microvoids are located near the surface in contact with the coagulation bath, and their removal can be achieved by increasing the concentration of DMAc beyond 70%. In the case of hollow fibers, the presence of DMAc in the coaxial coagulant promotes the formation of microvoids near the internal surface. Similar results were obtained using alcohols. The removal of these microvoids can only be effective at a high concentration of DMA (greater than 50%).

3.3. Properties of hollow fibers

Table 3 shows the main characteristics of hollow fibers. According to the table, the porosity of hollow fibers ranges from 77.67 to 79.16% for fibers 1-A to 1-D at a PSF concentration of 20 wt.%, and from 69.09 to 78.87% for fibers 2-A to 2-F at 25 wt.% PSF. The low porosity values are attributed to the rise in PSF concentration in the dope.

The injection rate of the coaxial coagulants influences the internal and external diameter of the hollow fibers. In the case of the hollow fibers of dope 1, using DMAc as bore fluid (1-B and 1-D), the internal and external diameters increase with the injection rate from 30 rpm to 50 rpm. Similarly, for the fibers of dope 2, using ethanol and DMAc as bore fluids, the internal and external diameters increase as the injection rate increases.

Bey et al. [27] reported that The flow rate of the bore fluid affects the internal diameter of PVDF hollow fibers. They observed that the thickness of these fibers decreases with the increasing flow rate of the bore fluid.

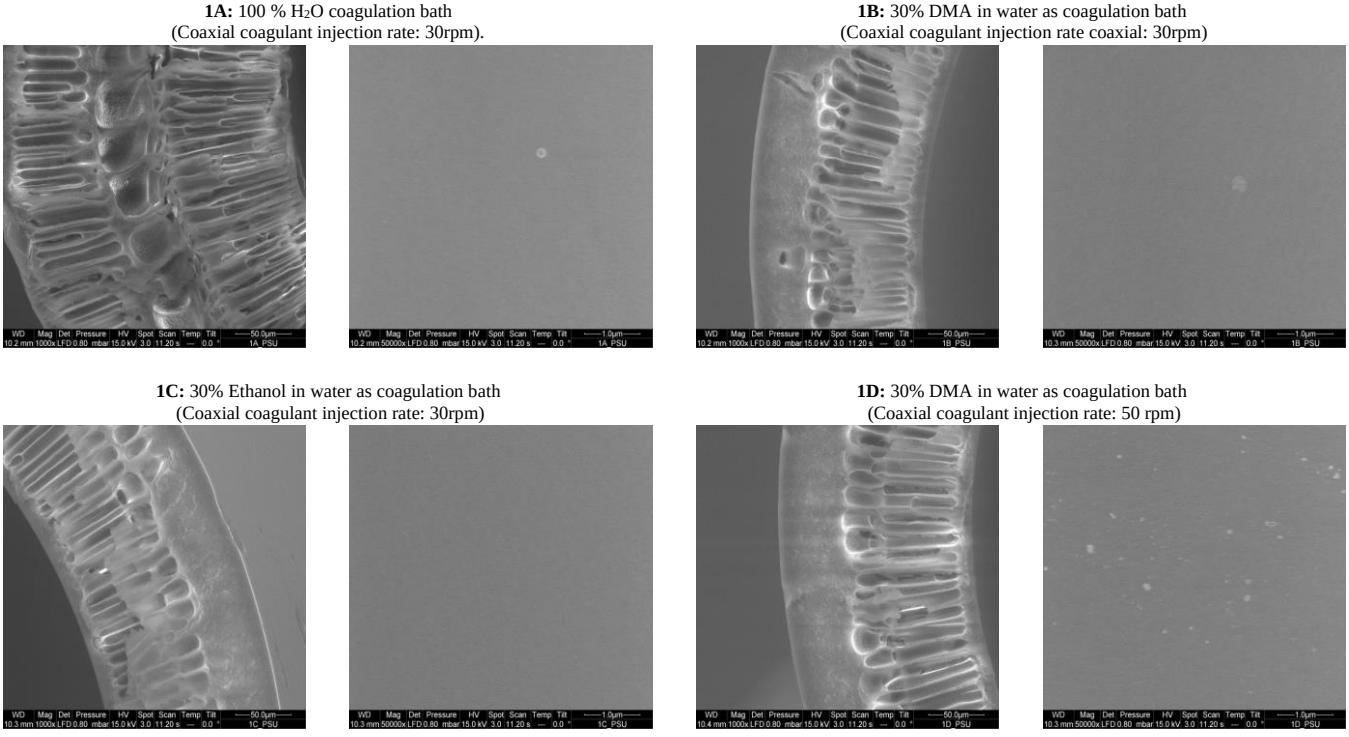

Fig. 3. SEM images of hollow fibers based on polysulfone PSF/PVP: 20%/15% (cross-section / inner surface)

2A: 100% H_2O coagulation bath
(Coaxial coagulant injection rate: 50 rpm)

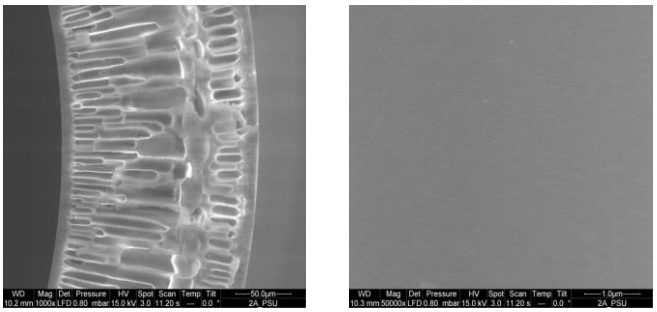

2B: 30% DMA in water as coagulation bath
(Coaxial coagulant injection rate: 50 rpm)

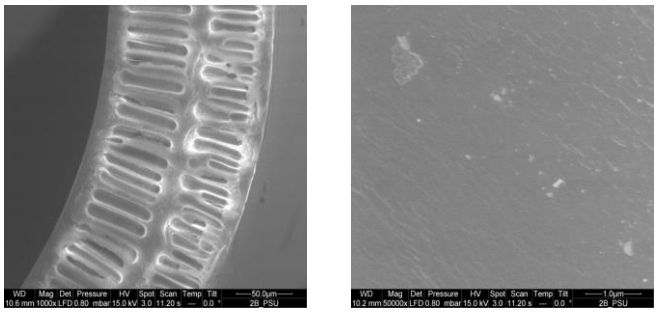

2C: 30% Ethanol in water as coagulation bath
(Coaxial coagulant injection rate: 50 rpm)

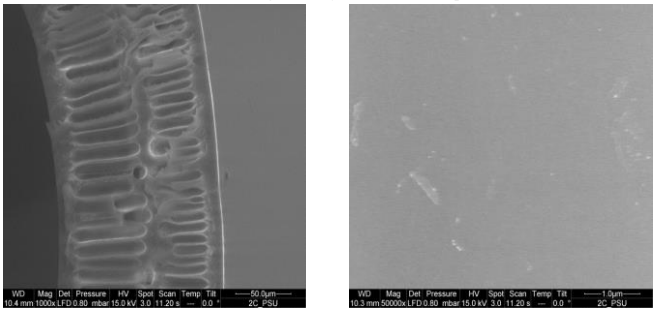

2D: 30% DMA in water as coagulation bath
(Coaxial coagulant injection rate: 70 rpm)

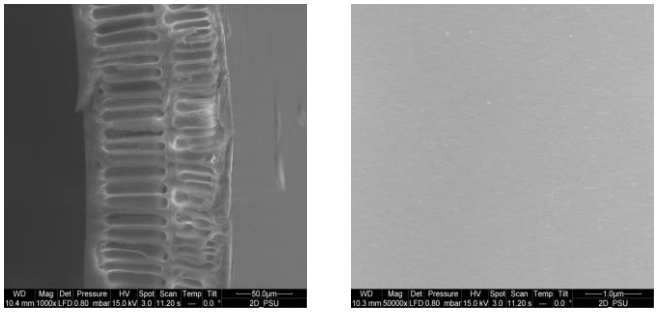

2E: 30% DMA in water as coagulation bath
(Coaxial coagulant injection rate: 30 rpm)

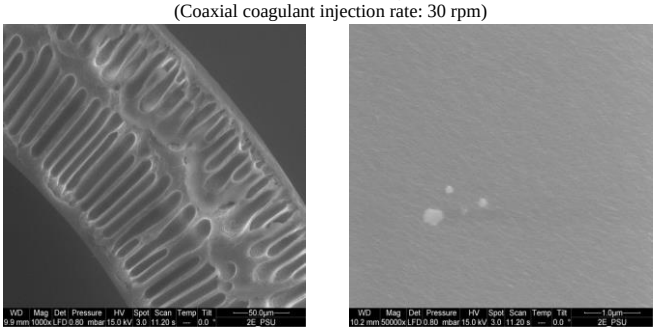

2F: 30% Ethanol in water as coagulation bath
(Coaxial coagulant injection velocity: 30rpm)

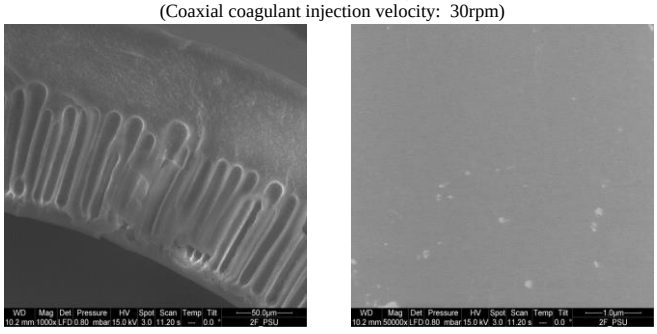

Fig. 4. SEM images of hollow fibers based on polysulfone PSF/PVP: 25%/10% (Cross-section / inner surface)

Table 3
Properties of hollow fibers based on PSF

Fiber	Polymer PSF	Additives	T (°C)	Coaxial coagulant and its velocity Composition /velocity	External diameter (mm)	Internal diameter (mm)	Thickness (mm)	Porosity (wet/dry) (%)	Membrane area (cm^2)
1-A	20 wt.%	PVP K-17 15%	50	H_2O 100% ;30 rpm	1.185	0.640	0.273	77.67	335
1-B				DMAc 30% ; 30 rpm	1.301	0.940	0.180	78.32	367
1-C				EtOH 30% ;30 rpm	1.318	0.870	0.224	78.86	372
1-D				DMAc 30% ; 50 rpm	1.393	0.990	0.202	79.16	393
2-A	25 wt.%	PVP K-17 10%	70	H_2O 100%; 50 rpm	1.499	1.150	0.175	78.87	423
2-B				DMAc 30% ; 50 rpm	1.527	1.150	0.188	74.02	431
2-C				EtOH 30% ;50 rpm	1.513	1.240	0.136	73.60	427
2-D				DMAc 30% ;70 rpm	1.578	1.270	0.154	73.49	446
2-E				DMAc 30% ; 30 rpm	1.343	0.99	0.177	69.09	379
2-F				EtOH 30% ; 30 rpm	1.381	0.9	0.240	71.18	390

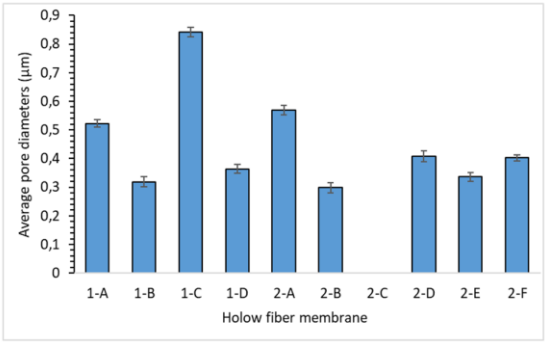

Fig. 5. Average pore diameter of hollow fibers.

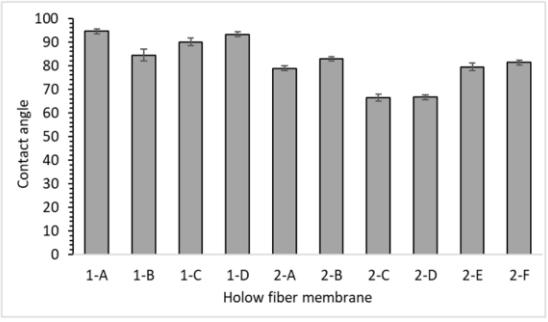

Fig. 6. Contact angle of hollow fibers.

According to Figs. 5 and 6, the hollow fibers spun from dope 1 have pore diameters ranging from 0.3 to 0.8 µm, with contact angles varying between 84.5-94.6 °. For dope 2, the pore diameters range from 0.35 to 0.55 µm, with contact angles between 66.4 and 82.9°. In fact, increasing the polymeric solution's viscosity delays the demixing of the membrane, leading to a reduction in pore diameter.

3.4. Mechanical tests

The mechanical characteristics of hollow fibers are related to their structure. The presence of microvoids gives low mechanical resistance to the membranes. Table 4 shows that the hollow fibers spun from dope 1 have a Young's modulus that ranges from 90.18 to 126.42 N/mm^2, a tensile strength varying from 3.97 to 5.22 N/mm^2, and an elongation at break between 42.07 to 51.25%. for the hollow fibers spun from dope 2, the elongation at break ranging from 49.13 to 69.04%, the tensile strength is between 6.56 to 9.65 N/mm^2, and the Young's modulus falls between 152.50 to 235.65 N/mm^2. The experimental findings demonstrate that mechanical properties increase when PSF concentration is raised from 20% to 25%. Moreover, as shown in the table, the mechanical properties decrease as porosity increases. This is due to the reduced volume fraction of polymer, which adversely affects the mechanical properties.

The results obtained are in line with the observation of Ismail et al. [32], who studied the effect of polymer concentration on mechanical properties at three different of amounts PSF (20, 25 and 30 wt.%). They reported that increasing the concentration of polymer results in higher elongation at rupture and tensile strength.

3.5. Extraction of chromium using spiral hollow fiber contactor

In this work, Extraction of chromium was performed. Type 2 spun hollow fibers were used to compare the performance of each membrane. The fibers of dope 1 have low stability, with phase dispersion appearing after just one hour of extraction. The results of the variation in chromium (VI) concentration as a function of time, the extraction efficiency, and the initial flux of the different hollow fibers are presented in Fig. 7 and Table 5, respectively. The 2-F membrane achieves the highest extraction performance, around 95%, with an initial flux of 3.8 × 10^{-6} mol/m².s. While the 2-A membrane has the lowest extraction rate 14%, with an initial flux of 1.5 × 10^{-7} mol/m².s. This shows that extraction performance depends on the membrane structure. Indeed, the 2-A membrane has microvoids throughout its cross-section, which resulted in a sharp drop in the extraction rate.

According to the literature, the results obtained in the present work are compared to those obtained with different systems. Table 6 summarizes some works.

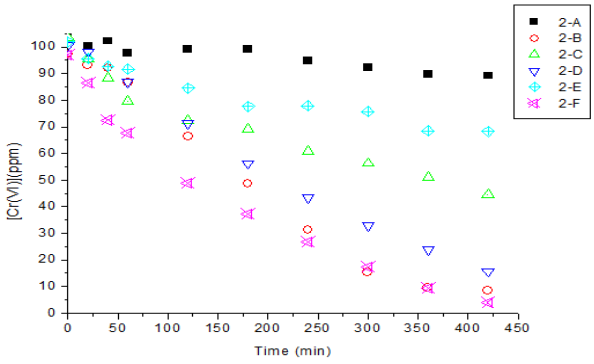

Fig. 7. Concentration of chromium (VI) as a function of time [Cr (VI)] = 100 ppm; [Aliquat 336] = 20%; T = 20°C; pH of the aqueous phase = 4.5; Time= 420 min; Flow rate= 10.8 ml/min.

Table 4
Mechanical properties of hollow fibers based on PSF.

Fiber	Polymer PSF	Additives	T (°C)	Coaxial coagulant and its velocity Composition /velocity	Emod N/mm²	Rm N/mm²	ebreak %
1-A	20 wt.%	PVP K-17 15 wt.%	50	H2O 100%, 30 rpm	117.17	4.82	42.07
1-B				DMAc 30%, 30 rpm	126.42	5.22	42.91
1-C				EtOH 30%, 30 rpm	107.67	4.53	51.25
1-D				DMAc 30%, 50 rpm	90.18	3.97	46.61
2-A	25 wt.%	PVP K-17 10 wt.%	70	H2O 100%, 50 rpm	152.50	6.56	49.13
2-B				DMAc 30%, 50 rpm	168.57	7.13	67.15
2-C				EtOH 30%, 50 rpm	231.78	9.61	61.30
2-D				DMAc 30%, 70 rpm	182.59	7.43	60.69
2-E				DMAc 30%, 30 rpm	235.65	9.65	64.46
2-F				EtOH 30%, 30 rpm	176.51	7.25	69.04

Table 5. Extraction efficiency and initial flux of Cr(VI) by PSF hollow fiber membranes [Cr (VI)] = 100 ppm; [Aliquat 336] = 20%; T = 20°C; pH of the aqueous phase = 4.5; Time= 420 min; Flow rate= 10.8 ml/min.

Hollow fiber membranes	Extraction efficiency (%)	Initial flux (×10^{-7}mol/m².s)
2-A	14	1.5
2-B	91	30
2-C	56	8.2
2-D	84	19
2-E	32	6.7
2-F	95	38

Table 6
Comparison of the transport of Cr(VI) through different membranes.

Membrane system	Chromium concentration (mol/l)	Feed solution pH	Carrier	Flux (µmol/m^2.s)	Reference
CTA-based PIM membrane	2.31×10^{-4}	1.2	Aliquat 336	3.11	[33]
Activated Composite Membrane	1×10^{-3}	1	Cyanex 923	3.03	[34]
Polymer inclusion membrane	1.8×10^{-6}	2	DOP/Aliquat-336	1.98×10^{-2}	[35]
Supported liquid membrane	1.8×10^{-6}	2	DOP/Aliquat-336	5.4×10^{-2}	[35]
Pore-filled membrane	1.8×10^{-6}	8	DABCO/PVBCl	6.66×10^{-2}	[35]
Electrodriven membrane extraction (Cr(VI)-PVCT$_{QAS}$)	1.923×10^{-3}	1.3	/	3.79	[36]
PVDF-based PIM membrane	$0{,}9\times10^{-3}$	3	Gd-glucaric acid	3	[9]
PSF- based PIM	9.62×10^{-6}	4	Aliquat 336	0.868	[37]
Spiral hollow fiber membrane contactor	1.923×10^{-3}	4.5	Aliquat 336	3.8	This work

3.6. Re-extraction of Cr (VI) through a spiral hollow fiber contactor

Chromium (VI) re-extraction from the organic phase containing Aliquat 336 loaded with Cr(VI) was studied using different stripping solutions: NaOH (0.05M), NaOH (0.1M), and NaCl (2M). The objective of this study is to regenerate the organic phase to allow its reuse in subsequent extraction cycles. The obtained results are presented in Fig. 8. The use of NaCl (2M) as the stripping phase shows a low re-extraction efficiency of 18%. By increasing the concentration of NaOH from 0.05M to 0.1M, the re-extraction efficiency of chromium (VI) significantly increased. At a NaOH concentration of 0.05M, the re-extraction efficiency is 39%. However, this concentration is insufficient to completely break down the Cr(VI)-Aliquat 336 complexes, leading to an accumulation of these complexes at the membrane-stripping interface, which hinders the transport of other complexes through the membrane. When the NaOH concentration is at 0.1M, the re-extraction efficiency reaches 92%, demonstrating the increased capability of NaOH at this concentration to break down the Cr(VI)-Aliquat 336 complexes, allowing optimal transport of chromium ions through the membrane.

It should be noted that many studies have used NaOH as the stripping phase for re-extracting chromium (VI), thus confirming its effectiveness in separation processes [38, 39]. Venkatesan and Palanivelu [40] reported that increasing the NaOH concentration leads to a higher re-extraction percentage until it reaches a maximum at 0.5M, then remains constant thereafter.

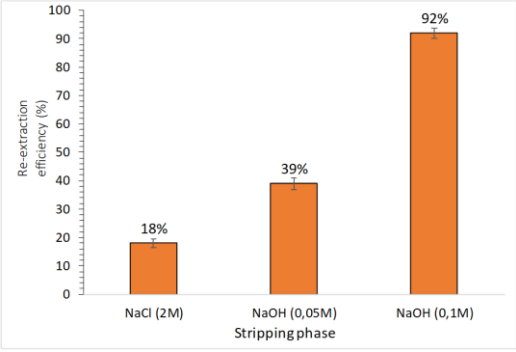

Fig. 8. Re-extraction of chromium (VI). [Cr (VI)] = 100 ppm; [Aliquat 336] = 20%; T = 20°C; pH of the aqueous phase = 4.5; Time= 420 min; Flow rate= 10.8 ml/min; Hollow fiber: 2-F.

4. Conclusions

Asymmetric and microporous hollow fibers PSf/PVP/DMF were prepared, with different polymer concentrations (20 wt.% and 25 wt.%). Viscosity analysis revealed that the dope solution's viscosity increased along with the PSF and PVP concentrations. As a result, the polymer solutions composed of 20% (PSF) / 15% (PVP) and 25% (PSF) / 10% (PVP) were found to be the most suitable for spinning. Furthermore, SEM micrographs indicated that raising the concentration of PSF from 20 to 25 wt.% had no effect on the fiber structure, and microvoids in the form of channels were observed. Several types of coaxial coagulants and the effects of their injection rate on the morphology and properties of the hollow fiber membranes were studied. It was found that increasing the injection rate of the coaxial coagulants improves their penetration into the polymer film, thus promoting the formation of microvoids. Additionally, experimental results from this study revealed that increasing the concentration of polymers significantly enhances the mechanical properties.

A specific type of hollow fiber membranes was used for the removal of Cr(VI) using a novel spiral hollow fiber contactor. The highest extraction efficiency was achieved at 95% with a feed phase concentration of 100 mg/L. Additionally, a re-extraction efficiency of 92% was attained using 0.1 M NaOH.

5. Acknowledgements

Our thanks to Dr Aoudia Sofiane for his help in carrying out this work and the means that have been made available to us for its outcome.

Data availability

No data was used for the research described in the article.

Funding

No funding was received for conducting this study. The authors have no relevant financial or non-financial interests to disclose.

CRedit authorship contribution statement

N. Zeghouati: Experiment and results discussion paper writing.
S. Bey: Conception of devices, discussion of results, supervisor and paper writing.
A. Belamri: Conception of the device on 3D printer.
A. Figoli: Results discussion, preparation and charactérization of membranes.
A. Criscuoli: Results analyses, discussion, preparation and charactérization of membranes.
M. Benamor: Results discussion and paper writing as a second supervisor.
E. Drioli: Results discussions.

Declaration of Competing Interest

The authors declare that they have no known competing financial interests or personal relationships that could have appeared to influence the work reported in this paper.

References

[1] F. Shen, J. Su, X. Zhang, K. Zhang, X. Qi, Chitosan-derived carbonaceous material for highly efficient adsorption of chromium (VI) from aqueous solution, Int. J. Biol. Macromol. 91 (2016) 443-449. DOI: 10.1016/j.ijbiomac.2016.05.103
[2] M. Amini, A. Rahbar-Kelishami, M. Alipour, O. Vahidi, Supported liquid membrane in metal ion separation: an overview, J. Membr. Sci. Res. 4 (2018) 121-135. DOI: 10.22079/JMSR.2017.63968.1138
[3] S. Tripathy, S. Sahu, R.K. Patel, R.B. Panda, P.K. Kar, Efficient removal of Cr(VI) by polyaniline modified biochar from date (Phoenix dactylifera) seed, Groundw. Sustain. Dev. 15 (2021) 100653. DOI: 10.1016/j.gsd.2021.100653
[4] I. Polowczyk, B.F. Urbano, B.L. Rivas, M. Bryjak, N. Kabay, Equilibrium and kinetic study of chromium sorption on resins with quaternary

ammonium and N-methyl-D glucamine groups, Chem. Eng. J. 284 (2016) 395–404. DOI: 10.1016/j.cej.2015.09.018
[5] D. Jia, Z. Jing, Y. Duan, J. Li, Ultrafast removal of Cr(VI) ions using polyamine modified carbon nanotubes, J. Taiwan Inst. Chem. Eng. 133 (2022) 104265. DOI: 10.1016/j.jtice.2022.104265
[6] Z. Ying, X. Ren, J. Li, G. Wu, Q. Wei, Recovery of chromium(VI) in wastewater using solvent extraction with amide, Hydrometall. 196 (2020) 105440. DOI: 10.1016/j.hydromet.2020.105440
[7] K. Dermentzis, K. Karakosta, C. Chatzichristou, T. Spanos, Comparing chemical coagulation and electrocoagulation on removal efficiency of chromium (VI) from galvanic effluents, J. Eng. Sci. Technol. Rev. 14 (2021) 54 – 58. DOI: 10.25103/jestr.142.07
[8] N.S. Rathore, A.M. Sastre, A.K. Pabby, Membrane assisted liquid extraction of actinides and remediation of nuclear waste: a review, J. Membr. Sci. Res. 2 (2016) 2-13. DOI: 10.22079/JMSR.2016.15872
[9] Z. Habibi, C. Youssef, M. Riri, S. Majid, K. Touaj, M. Hlaibi, A novel polymer inclusion membrane containing an organometallic complex carrier for the extraction and recovery of chromium and nickel from wastewater, J. Membr. Sci. Res. 9 (2023) 546447. DOI: 10.22079/JMSR.2022.546447.1527
[10] S. Bensaadi, N. Drai, O. Arous, Y. Berbar, Z.E. Hammache, M. Amara, B. Van der Bruggen, A study of chromium (VI) ions fixation and transport using polymer inclusion membrane containing D2EHPA as complexing agent, J. Membr. Sci. Res. 8 (2022) 531653. DOI: 10.22079/JMSR.2021.531653.1470
[11] S. Kavitha, S.S. Baral, S. Ganesan, Removal of hexavalent chromium using emulsion liquid membrane with jet mixer: a continuous approach, Chem. Eng. Technol. 46 (2023) 934-939. DOI: 10.1002/ceat.202200183
[12] C.F. Wan, T. Yang, G.G. Lipscomb, D.J. Stookey, T.S. Chung, Design and fabrication of hollow fiber membrane modules, J. Membr. Sci. 538 (2017) 96-107. DOI: 10.1016/j.memsci.2017.05.047
[13] A. Mansourizadeh, I. Rezaei, W.J. Lau, M.Q. Seah, A.F. Ismail. A review on recent progress in environmental applications of membrane contactor technology, J. Environ. Chem. Eng. 10 (2022) 107631. DOI : 10.1016/j.jece.2022.107631
[14] N. Ghasem, Modeling and simulation of CO2 absorption enhancement in hollow-fiber membrane contactors using CNT–water-based nanofluids, J. Membr. Sci. Res. 5 (2019) 295-302. DOI: 10.22079/JMSR.2019.100177.1239
[15] G. Bakeri, A comparative study on the application of porous PES and PEI hollow fiber membranes in gas humidifcation process, J. Membr. Sci. Res. 5 (2019) 11-19. DOI: 10.22079/JMSR.2018.71014.1156
[16] T.Y. Cath, S. Gormly, E.G. Beaudry, M.T. Flynn, V.D. Adams, A.E. Childress, Membrane contactor processes for wastewater reclamation in space: part I. Direct osmotic concentration as pretreatment for reverse osmosis, J. Membr. Sci. 257 (2005) 85-98. DOI: 10.1016/j.memsci.2004.08.039
[17] N.H. Othman, A. Md Noor, M.S.A. Yusoff, P.S. Goh, A.F. Ismail, Effect of ethylene glycol as pore former on polyphenylsulfone hollow fiber membrane for crude palm oil deacidification through membrane contactor, J. Membr. Sci. Res. 3 (2017) 291-295. DOI: 10.22079/JMSR.2016.21596
[18] G.B. Kim, S.J. Kim, M.H. Kim, C.U. Hong, H.S. Kang, Development of a hollow fiber membrane module for using implantable artificial lung, J. Membr. Sci. 326 (2009) 130-136. DOI: 10.1016/j.memsci.2008.09.045
[19] X. Yang, R. Wang, A.G. Fane, C.Y. Tang, I.G. Wenten, Membrane module design and dynamic shear-induced techniques to enhance liquid separation by hollow fiber modules: a review, Desalination Water Treat. 51 (2013) 16-18. DOI: 10.1080/19443994.2012.751146
[20] J. Chen, C. Zhou, B. Xie, J. Zhang, Simulation of the enhancement of Dean flow on the liquid–liquid extraction in membrane contactors, Sep. Purif. Technol. 285 (2022) 120384. DOI: 10.1016/j.seppur.2021.120384
[21] M.H. Weissman, L.F. Mockros, Gas transfer to blood flowing in coiled tubes, J. Eng. Mech. Div. 94 (1968) 857. DOI: 10.1061/JMCEA3.0000991
[22] L. Liu, L. Li, Z. Ding, R. Ma, Z. Yang, Mass transfer enhancement in coiled hollow fiber membrane modules, J. Membr. Sci. 264 (2005) 113-121. DOI: 10.1016/j.memsci.2005.04.035
[23] Š. Schlosser, E. Sabolova, Three-phase contactor with distributed U-shaped bundles of hollow-fibers for pertraction, J. Membr. Sci. 210 (2002) 331-347. DOI: 10.1016/S0376-7388(02)00408-8
[24] Q. Kong, Y. Zhang, H. Tian, L. Fang, M. Zhou, L. Zhu, B. Zhu, Mass transfer enhancement of hollow fiber membrane deoxygenation by Dean vortices, J. Zhejiang Univ. Sci. A. 20 (2019) 601-613. DOI: 10.1631/jzus.A1900181
[25] J.N. Ghogomu, C. Guigui, J.C. Rouch, M.J. Clifton, P. Aptel, Hollow-fibre membrane module design: comparison of different curved geometries with Dean vortices, J. Membr. Sci. 181 (2001) 71-80. DOI: 10.1016/S0376-7388(00)00364-1
[26] K. Sofiya, E. Poonguzhali, A. Kapoor, P. Delfino, S. Prabhakar, Separation of carboxylic acids from aqueous solutions using hollow fiber membrane contactors, J. Membr. Sci. Res. 5 (2019) 233-239. DOI: 10.22079/JMSR.2018.88804.1199
[27] S. Bey, A. Criscuoli, A.Figoli, A. Leopold, S. Simone, M. Benamor, E. Drioli, Removal of As(V) by PVDF hollow fibers membrane contactors using Aliquat-336 as extractant, Desalination. 264 (2010) 193-200. DOI: 10.1016/j.desal.2010.09.027
[28] S. Simone, A. Figoli, A. Criscuoli, M.C. Carnevale, A. Rosselli, E. Drioli, Preparation of hollow fibre membranes from PVDF/PVP blends and their application in VDM, J. Membr. Sci. 364 (2010) 219-232. DOI: 10.1016/j.memsci.2010.08.013
[29] S. Mansur, M.H.D. Othman, A.F. Ismail, M.N.Z. Abidin, N. Said, P.S. Goh, H. Hasbullah, S.H.S. Abdul Kadir, F. Kamal, Study on the effect of PVP additive on the performance of PSf/PVP ultrafiltration hollow fiber membrane, Malays. J. Fundam. Appl. Sci. 14 (2018) 343-347.
[30] M.J. Han, S.T. Nam, Thermodynamic and rheological variation in polysulfone solution by PVP and its effect in the preparation of phase inversion membrane, J. Membr. Sci. 202 (2002) 55–61. DOI: 10.1016/S0376-7388(01)00718-9
[31] P.S.T. Machado, A.C. Habert, C.P. Borges, Membrane formation mechanism based on precipitation kinetics and membrane morphology: flat and hollow fiber polysulfone membranes, J. Membr. Sci. 155 (1999) 171-83. DOI: 10.1016/S0376-7388(98)00266-X
[32] N.M. Ismail, N.R. Jakariah, N. Bolong, S.M. Anissuzaman, N.A.H.M. Nordin, A.R. Razali, Effect of polymer concentration on the morphology and mechanical properties of asymmetric polysulfone (PSf) membrane, J. Appl. Membr. Sci. Technol. 21 (2017) 33-41. DOI: 10.11113/amst.v21i1.107
[33] O. Kebiche-Senhadji, S. Tingry, P. Seta, M. Benamor, Selective extraction of Cr(VI) over metallic species by polymer inclusion membrane (PIM) using anion (Aliquat 336) as carrier, Desalination. 258 (2010) 59-65. DOI: 10.1016/j.desal.2010.03.047
[34] G. Arslan, A. Tor, H. Muslu, M. Ozmen, I. Akin, Y. Cengeloglu, M. Ersoz, Facilitated transport of Cr (VI) through a novel activated composite membrane containing Cyanex 923 as a carrier, J. Membr. Sci. DOI: 10.1016/j.memsci.2009.03.049
[35] Y.M. Scindia, A.K. Pandey, A.V.R. Reddy, Coupled-diffusion transport of Cr(VI) across anion-exchange membranes prepared by physical and chemical immobilization methods, J. Membr. Sci. 249 (2005) 143-152. DOI: 10.1016/j.memsci.2004.10.015
[36] X. Meng, W. Li, Y. Tian, C. Sun, J. Huang, X. Liu, Synthesis of trioctyl polyvinyl chloride ammonium, membrane extraction properties, and electrodriven mass transfer behavior of chromium (VI), Sep. Purif. Technol. 320 (2023) 124191. DOI: 10.1016/j.seppur.2023.124191
[37] P. Kunene, O. Akinbami, N. Motsoane, H. Tutu, L. Chimuka, H. Richards, Feasibility of polysulfone as base polymer in a polymer inclusion membrane: synthesis and characterisation, J. Membr. Sci. Res. 6 (2020) 203-210. DOI: 10.22079/JMSR.2019.111596.1278
[38] F. Sellami, O. Kebiche-Senhadji, S. Marais, L. Colasse, K. Fatyeyeva, Enhanced removal of Cr(VI) by polymer inclusion membrane based on poly(vinylidene fluoride) and Aliquat 336, Sep. Purif. Technol. 248 (2020) 117038. DOI: 10.1016/j.seppur.2020.117038
[39] Y. Guo, H.Y. Li, Y.H. Yuan, J. Huang, J. Diao, B. Xie, Microemulsion extraction: an efficient way for simultaneous detoxification and resource recovery of hazardous wastewater containing V(V) and Cr(VI), J. Hazard. Mater. 386 (2020) 121948. DOI: 10.1016/j.jhazmat.2019.121948
[40] P. Venkateswaran, K. Palanivelu, Studies on recovery of hexavalent chromium from plating wastewater by supported liquid membrane using tri-n-butyl phosphate as carrier, Hydrometall. 78 (2005) 107-115. DOI: 10.1016/j.hydromet.2004.10.021